The (Current) Acridine Solid Form Landscape: Eight Polymorphs and a Hydrate

Einat Schur[a], Joel Bernstein[,a,b§], Louise S. Price[c], Rui Guo[c], Sarah L. Price[c], Saul H. Lapidus[d†],

Peter W. Stephens*,[d]

[a] Department of Chemistry, Ben-Gurion University of the Negev, Beer Sheva, Israel

[b] Faculty of Science, New York University Abu Dhabi, Abu Dhabi, United Arab Emirates

[c] Department of Chemistry, University College London, 20 Gordon Street, London WC1H 0AJ
U.K.

[d] Department of Physics and Astronomy, Stony Brook University, Stony Brook, NY 11794-3800

SYNOPSIS

The simple planar molecule acridine is polymorphically promiscuous, with, at latest count, eight

distinct unsolvated forms, and one hydrate. This makes it a compelling model system to study its

polymorphism, as this represents a challenge to our understanding of crystallization.

I. Introduction

Polymorphism, the occurrence of more than one distinct crystal structure of a particular molecule, is a phenomenon of great scientific and economic interest. One generally speaks of polymorphs (as opposed to structural phase transitions) in cases where the various forms are stable, or metastable, so that they do not readily interconvert on time scales of days or longer. Beside intrinsic scientific interest, polymorphism can lead to significant differences in the performance of many materials; examples of troublesome appearance of polymorphs include pharmaceuticals and chocolate.[1,2] While many polymorphic systems have been studied, predictive systematics are lacking; it is currently not possible to make a good guess which molecules will have several accessible polymorphs, and they will be discovered only through a rather tedious search in the laboratory, which nowadays can be complemented by computer modeling.

Acridine was first isolated in 1870, and was known to be crystalline well before Kofler's hot stage microscope studies revealed five forms, including crystal habit, phase transitions, and melting points all between 106-110 °C.[3] Subsequent studies, prior to our work, have turned up seven anhydrous forms, of which the crystal structures were known of five, and one hydrate.[4-14] Over the years, inconsistent naming of the solid forms has led to confusion in characterizing, distinguishing, and identifying the various solid forms. The nomenclature in this review is consistent with forms identified in the 2019 edition of the Cambridge Crystal Structure Database.[15] Table 1 summarizes the currently known solid forms, their lattices, and how they are named in other work.

Table 1. Crystal forms of acridine and their designation in various publications. Space groups and lattice parameters are given in the published settings, which are not always the standard ones. Ambient temperature except as noted. CSD refcodes are given for all published structures; in bold face for lattice parameters listed here. Entries in italics contain crystallographic data only as literature citations. Entries in red represent different designations of the crystal forms than those used here or in the CSD.

	I (acridine 0.75 hydrate)	II	III	IV	V	VI	VII	VIII	IX
Space Group	*Pbcn*	*P2₁/n*	*P2₁/c*	*P2₁2₁2₁*	*Aa* [a]	*Cc*	*P2₁/n*		*P2₁/n*
a (Å)	26.400(5)	11.2527(10)	6.0693(4)	6.1788(5)	20.04	6.174(2)	6.0569(10)		11.2845(1)
b (Å)	8.893(5)	5.9510(5)	18.8181(7)	15.7185(16)	5.95	23.497(8)	22.813(4)		12.3818(1)
c (Å)	17.492(5)	13.6018(12)	16.2830(5)	29.312(3)	16.37	12.868(4)	13.204(2)		6.6791(1)
β (°)	–	99.527(2)	95.155(3)	90	110.63	96.483(6)	95.938(4)		92.062(1)
Z,Z'	16, 2	4, 1	8, 2	12, 3	8, 2	8, 2	8, 2		4, 1
Lowde *et al.*[4]	I	III	II						
Phillips[5]		III ACRDIN01							
Phillips *et al.*[6]			II ACRDIN						
Herbstein and Schmidt[7]	γ		α	δ ACRDIN03[b]	β **ACRDIN02**[b]				
Clarke *et al.*[8]	*I*	***III***	*II*	*IV*	*V*				
Mei and Wolf[9]		**II ACRDIN04**[c]	*III*	*IV*	*V*	VI **ACRDIN05**[c]	VII **ACRDIN06**[c]		
Braga *et al.*[10]		*II*	III **ACRDIN07**	IV **ACRDIN08**				VIII ¶	
Kupka *et al.*[11]		*II*	III ACRDIN09 ACRDIN10	*IV*	*V*	*VI*	*VII*		
Lusi *et al.*[12]		III ACRDIN11	*II*						
Schur *et al.*[13]	**ZZZRLO01**								
Schur[17]	Hydrate	III	II	IV	V	VI	VII	*VIII*	IX
Stephens *et al.*[14]									IX **1869547**

a) Listed lattice parameters are from CSD ACRDIN02. Herbstein and Schmidt publication has $a = 16.37(4)$ Å, $b = 5.95(2)$ Å, $c = 30.01(10)$ Å, $\beta = 141.33(50)°$, space group *Aa*, which is not equivalent.

b) No atomic coordinates given.   c) 185−188 K

The importance of mapping the solid form landscape, especially for a newly prepared compound of potential commercial use, has led to the common practice of a "polymorph screen." The strategy for designing and executing such a screen will necessarily differ for every compound. We are not aware of any such attempt for acridine. We summarize the literature of reported crystallization experiments in Table S1, which clearly demonstrates that the so-called *occurrence domain* for many of the forms is not uniquely defined. Indeed, there are apparently similar or identical conditions that lead to different forms or a mixture of concomitant forms, complicating and confusing their identification and characterization.

Currently, the computational prediction of crystal structures is being developed as a complementary method to aid experimental exploration of the solid form landscape.[16] This review grew from coordinated experimental and computational efforts to map the solid form landscape of acridine,[17] and to search for the lowest energy crystal structures of this simple, rigid molecule. Interestingly, the structure computed to have the lowest energy had not been experimentally observed at the outset of this work, and the experiments turned up a previously unknown phase that turned out to match the predicted structure, now designated form IX.[14]

II. Structures of Acridine Anhydrate Phases

The first identified crystal form of acridine was described by Groth in 1919.[18] Notwithstanding the fact that it was subsequently (1953) identified as a hydrate,[4] it is commonly referred to as form I; its structure was not determined until 2011.[13] It is not stable in air at ambient temperature, converting to forms II and/or III.

All known crystalline forms of acridine are summarized in Table 1. Presumably, Kofler's initial study found forms I-V, although there is no direct confirmation. Even though single

crystals of form V were described by Herbstein and Schmidt,[7] no information beyond lattice parameters and space group were published, and while it was evidently reproduced once,[8] there has been no subsequent report of its existence or structure. Likewise, form VIII was only observed by powder x-ray diffraction[10] in a mixture with form II, without a structure determination. Of the crystallographically characterized structures, four have space group $P2_1/c$ (or the alternative $P2_1/n$ setting), one is in the chiral group $P2_12_12_1$, and one in the polar group Cc.

Two of the forms, VI and VII, were discovered in a study of the influence of certain dicarboxylic acids in solution during crystallization, motivated by the possibility of using a templating effect to create new crystal forms.[9] In that work, it was hypothesized that transient absorption of those molecules in solution on the surface of the growing crystal inhibited the formation of more stable forms. However, forms VI and VII also turned up in a polycrystalline mixture formed by quenching molten acridine, as described in the SI Table S3. Form VII was also observed when an acetone solution was crash-cooled in a study of solvent effects.[19]

While all information about packing geometry is embodied in the crystal structure, it is not easy to grasp details of intermolecular interactions in three dimensions by directly viewing projections. For that purpose, the recently developed method of Hirshfeld surfaces and their fingerprints tends to be much more informative. The Hirshfeld surface (HS) of a given molecule in a crystal is defined as the boundary of space where the crudely approximated electron density of the molecule exceeds the electron density of the other molecules.[20,21] For simplicity of computation and to avoid ambiguity of the definition, this is computed assuming spherical, free atom electron densities. HS's divide the volume of the crystal into smooth molecular regions, with small intermolecular voids. Various information can be encoded by coloring the HS; in this

review we color by d_{norm}, the contact distance normalized to the sum of van der Waals radii.[22] A further development is the Hirshfeld fingerprint plot (HFP), which is a two-dimensional histogram of the distance to the nearest internal atom, d_i, and the nearest external atom, d_e, for each point on the surface.[23] This is colored according to the fraction of the surface area covered by points with that (d_i, d_e) value, ranging from blue (small) through green, to red (large). Insofar as these tools are best explained with examples, we proceed to consider acridine form II, one of two structures with only one molecule in the irreducible cell.

Fig. 1a shows four symmetry-equivalent molecules in the unit cell of form II, lying roughly in a line along the [111] direction. The long axes of all molecules in the crystal are nearly parallel. The closest intermolecular contacts are C⋯H distances of 2.76 Å and 2.84 Å, indicated by salmon-colored bonds, which are less than the sum of the van der Waals radii (1.70 Å + 1.20 Å). In this review, we will call any intermolecular pair of atoms "weakly bonded" if their distance is less than the sum of the van der Waals radii. The distance between the (parallel) planes of the two molecules in the center of the drawing is 3.45 Å; there is a lateral shift of 1.85 Å between the two molecules, suggesting a significant π-π interaction as well. The HS, illustrated in Fig. 1b, conforms to the shape of the molecule as expected. In this view, it is colored according to d_{norm}, so that the two red spots indicate regions of the surface closest to the C and H atoms with the 2.76 Å contact. The red spots of the HS's would be in contact in the crystal. The HS encloses a volume of 219.4 Å^3, compared with the crystal's molar volume of 224.6 Å^3, illustrating the general result that there is very little (in this case, 2.3%) void space between the HS's in a typical molecular solid.
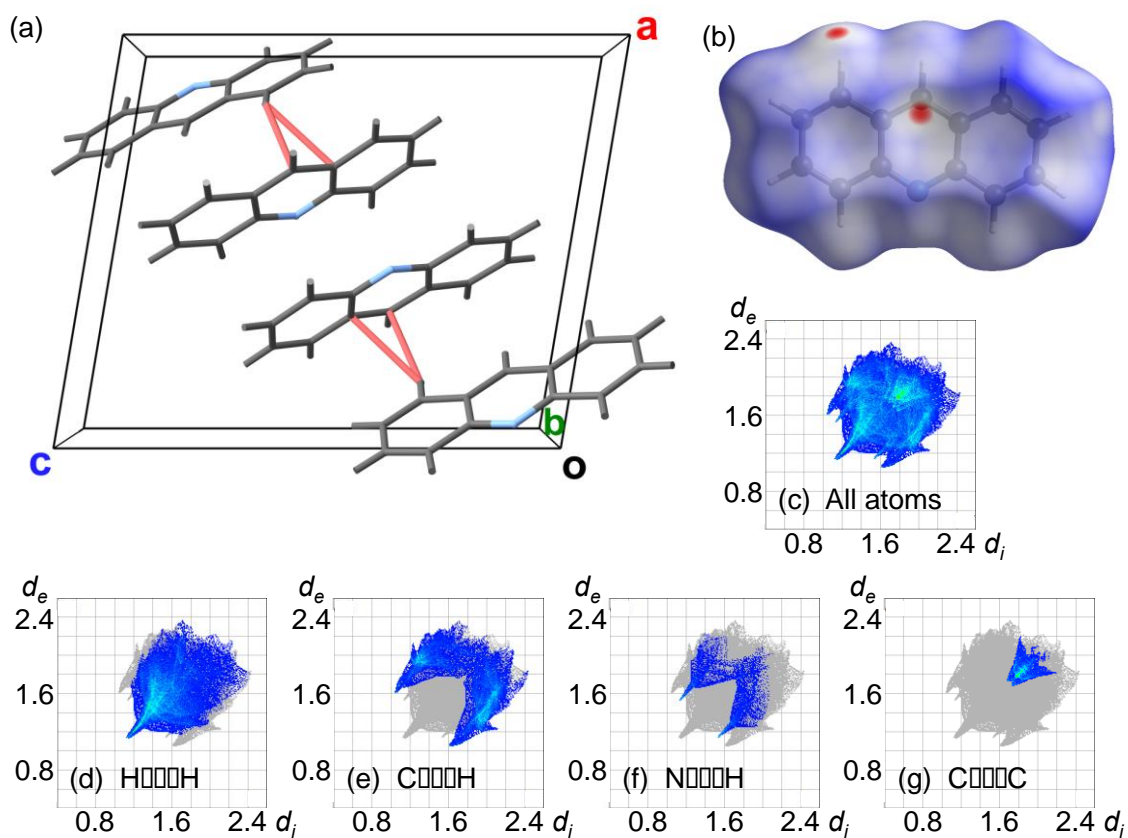
Figure 1. Representations of the structure of acridine form II ($P2_1/n$, $Z'=1$). (a) Stick model of crystal structure.[9,24] C and H atoms are depicted in grey, N is blue. The salmon-colored lines represent contacts between atoms that are closer than the sum of their van der Waals radii. (b) Hirshfeld surface of a molecule, shaded according to d_{norm}.[25] (c) Hirshfeld fingerprints of all atoms and (d-g) specific atom pairs on the grey background of all atom interactions.[25] In (e) and (f) the region above the diagonal generally has an internal H atom in contact with an external C or N atom respectively.

Fig. 1c shows the HFP of form II. This illustrates the general reflection symmetry of HFP's about the $d_i = d_e$ diagonal in $Z' = 1$ structures, because nearly every point on the HS of a given molecule has a corresponding point, with d_i and d_e reversed, on the HS of its immediate neighbor. It is possible to prepare a HFP restricted to particular atoms, as illustrated for intermolecular H···H connections in Fig. 1d. Fig. 1e and 1f show C···H and N···H interactions respectively. Fig. 1g illustrates the partial HFP for C···C interactions, which can largely be classified as π-π interactions, because the molecule is essentially planar, with edges protected by H atoms.

The only other known form of acridine with a single molecule in the irreducible cell ($Z' = 1$) is form IX, predicted and discovered by the research program that inspired this review. Its structure, HS, and HFP are illustrated in Fig. 2. Here we see that, unlike form II, the long axes of the molecules are not aligned in a common direction. It is noteworthy that the four symmetry-equivalent molecules are connected by a cyclic set of C···H and N···H interactions. Relative to form II, form IX shows closer H···H interactions, but less close C···H and C···C interactions, evidently due to less π stacking in this structure.
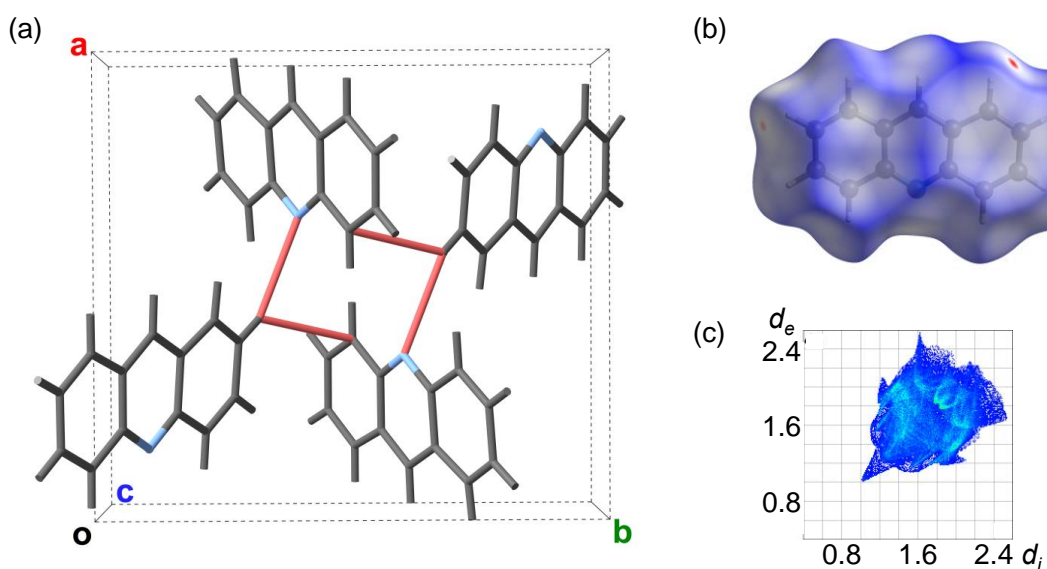
Figure 2. Representations of the structure of acridine form IX ($P2_1/n$, $Z'=1$).[14]   Shadings as used in Fig. 1.   Two intermolecular contacts are visible in the HS in Fig. 2b.   The more prominent one at the upper right is a 2.29 Å H···H interaction not shown in Fig. 2a; the one at the left indicates the contact between the internal H atom and adjacent C and N atoms. Fig. 2c is the all atom HFP plot.

Acridine form III, which is the end product when other forms are heated, has a structure consisting of two inequivalent molecules. The structure consists of columns along the *a*-axis, with two each of the two molecules, with their long axes in the *b-c* plane, roughly parallel in each column (Fig. 3a,). Molecule 1 has close contacts to both molecules, whereas molecule 2 has a rather different environment, with weak bonds only to molecule 1. The HS and HFP of molecule 1 in Figs. 3c and 3d show the close connections of the C and H atoms to molecule 2; their image is apparent on the HS of molecule 2 (Fig. 3e). The opposite side (not shown) of the HS of molecule 1 likewise shows close interaction of the N and adjacent H atoms to their inversion partners in molecule 1.
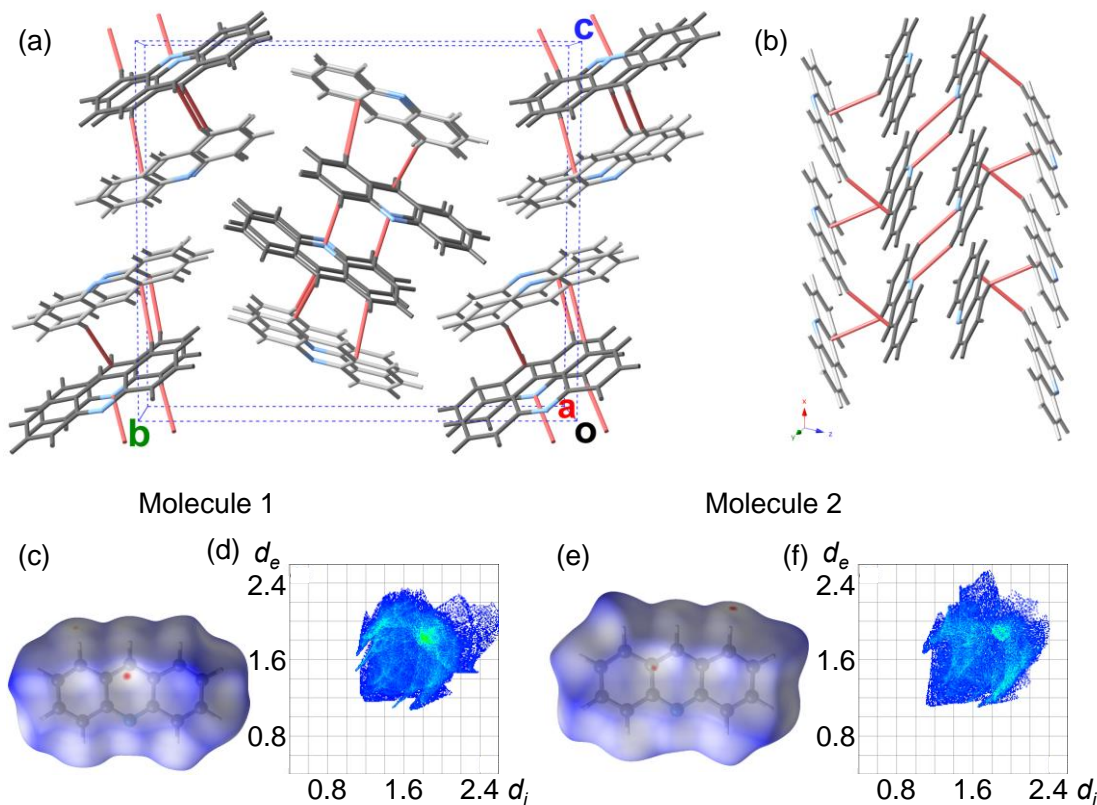
Figure 3. Representations of the structure of acridine form III ($P2_1/c$ $Z'=2$).[10] In panels (a,b), molecule 1 has a darker shade of grey, and molecule 2 is lighter; N is blue, and the salmon-colored lines represent pairs of atoms that are closer than the sum of their van der Waals radii. One side of each HS and all atom HFP are shown for the two independent molecules.

Form VII has the same monoclinic space group with two inequivalent molecules, and a very similar topology to form III, as shown in Figs. 4a and 4b. Likewise, the HS and HFP plots of form VII are similar to those of form III despite the cell parameters being different.
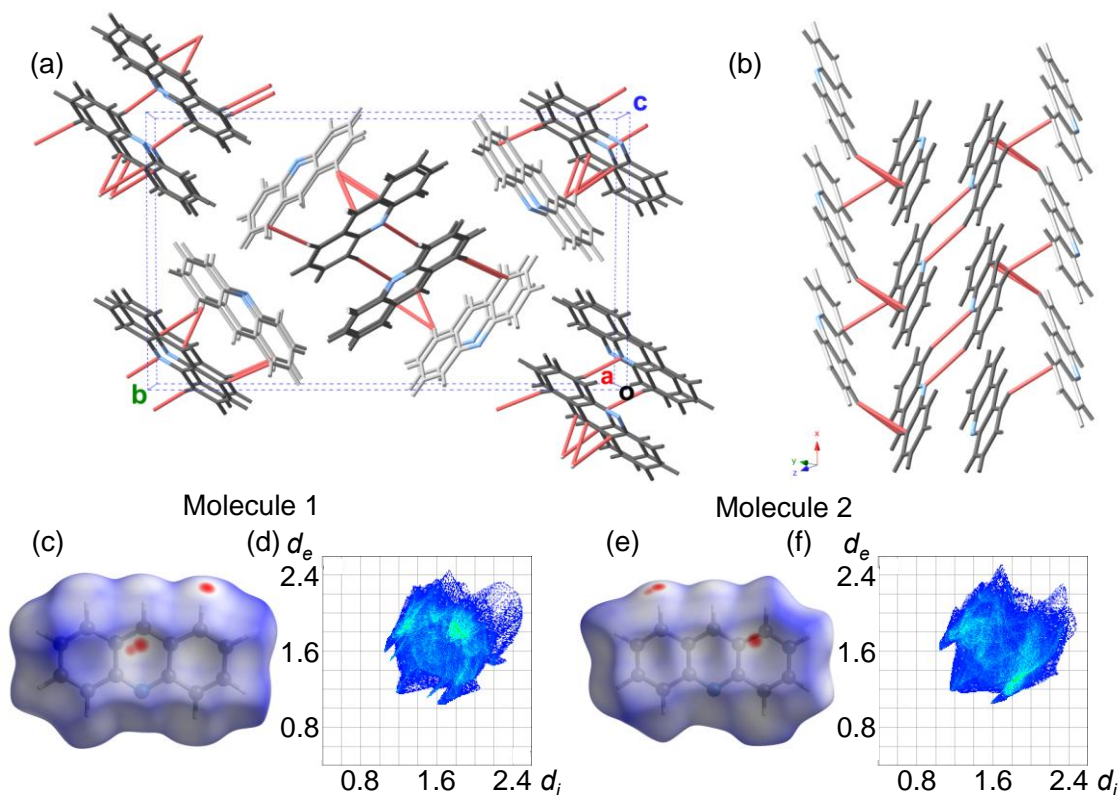
10

Figure 4. Structure of acridine form VII ($P2_1/n$, Z'=2).[9] Shadings as used in Fig. 3.

Form VI is unique in that it is polar; in every molecule, the N atom is close to the −**a** direction relative to the center, leading to a net dipole moment of the unit cell. Its structure, shown in Fig. 5a, is more complicated than the phases discussed so far. Unlike any other phase, weak bonds extend throughout the crystal in three dimensions. Both molecule 1 (dark) and molecule 2 (light) are weakly bonded with both molecules. Figs. 5b-5g show that molecule 1 interacts primarily through contacts out of its molecular plane, whereas close contacts to molecule 2 occur primarily to the H atoms at its edges.
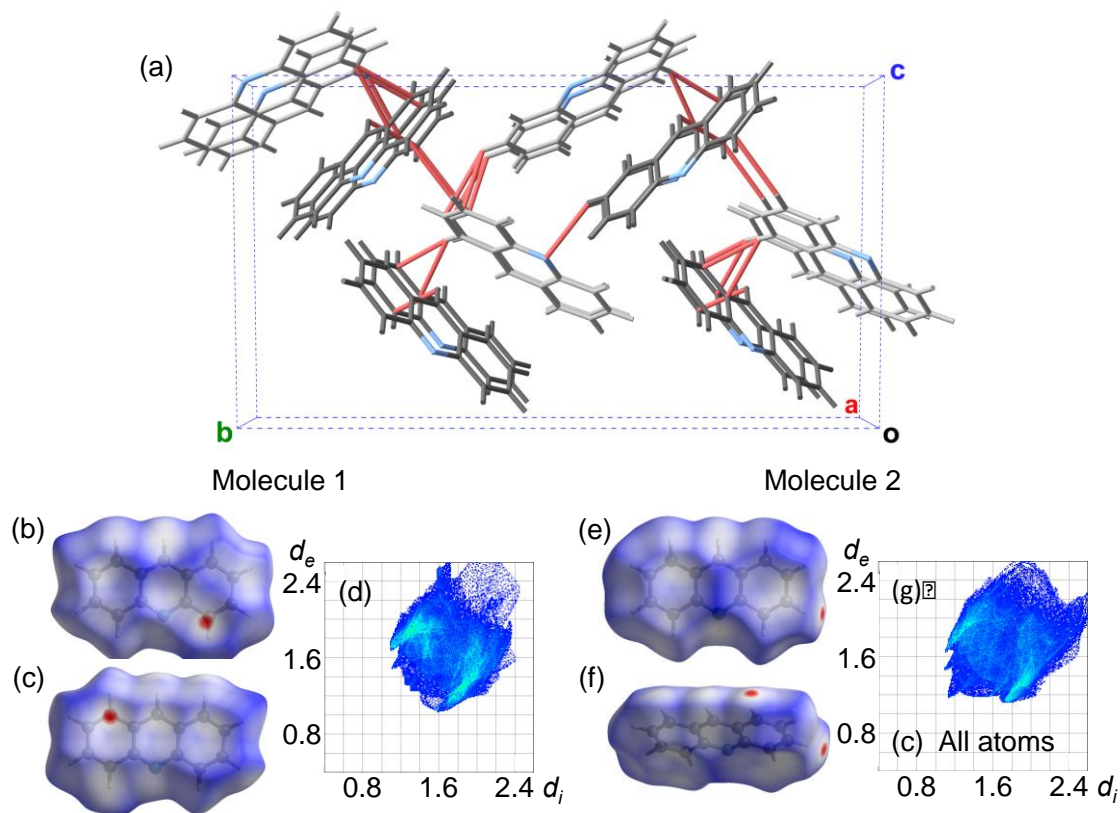
Figure 5. Structure of acridine form VI (*Cc Z'*=2).[9] Shadings as used in Fig. 3. Note that the N atoms are all pointing out of the page. Two views are given of each HS to show all short contacts.

Crystallographically, the most complicated form of acridine is IV, which has three independent molecules in the $P2_12_12_1$ orthorhombic unit cell. The weakly bonded groups of molecules occur in chains along the *a*-axis, with six molecules in each link (Fig. 6a). The structure of the chains is visible in Fig. 6b, where molecule 3 has been removed for clarity. Molecule 1 holds the structure together, weakly bonded to other copies of itself in a corkscrew along the 2_1 screw axis along *a*. Molecule 2 reinforces this column, bridging two copies of molecule 1 with weak C···H bonds, and molecule 3 bonds to molecule 1 with a weak N···H bond. The HS and HFP plots for

each molecule in form IV (Figs. 6c-6i) emphasize the very different environment of each molecule. Planar molecules with an additional mirror, such as acridine, are unusual in acentric space groups, but not unknown; 2,3-dichloroanthraquinone[26] in $P2_12_12_1$ and phenanthrene[27] in $P2_1$ are other examples.
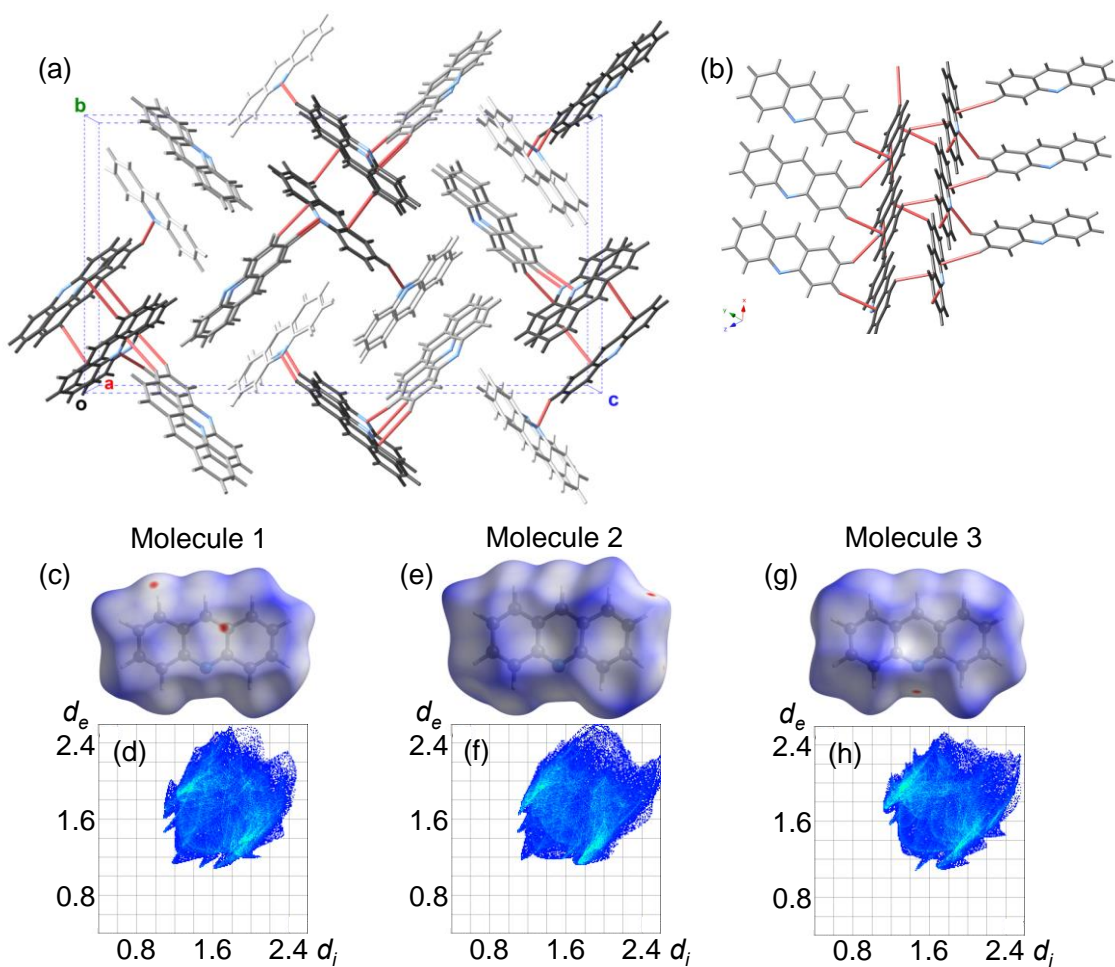

Figure 6. Structure of acridine form IV ($P2_12_12_1$, Z'=3).[10] In panel (a) molecule 1 is darkest, molecule 2 is intermediate, and molecule 3 is lightest. (b) shows the chain structure with molecule 3 removed for clarity.

Fig. 7 shows the fraction of the HFP allocated to each pair of intermolecular interactions (H···H, C···H, etc.) for each molecule in all forms for which the structures are known, concisely summarizing the range of local environments of acridine molecules in these polymorphs. In all

13

cases, most of the surface is made up of H···H (41-52 %) and C···H (33-49 %) contacts, with between 7% and 12% of the area in N···H contacts. These might be regarded as weak hydrogen bonds, with the H donated by its covalently bonded C atom. The N···H distances range from 2.66 to 2.83 Å, compared with the 2.75 Å sum of van der Waals radii. We note that CH···N interactions with N···H distances in the range of 2.57 – 2.74 Å and computationally estimated energies in the range -11.2 to -14.4 kJ/mol were discussed as significant factors in the polymorphism of a flexible CHN compound.[28] In acridine, the largest variation among forms is in the C···C contacts (0.1 to 8 %), which, as a rough measure of the variation in π-π interactions, is also likely to be significant.
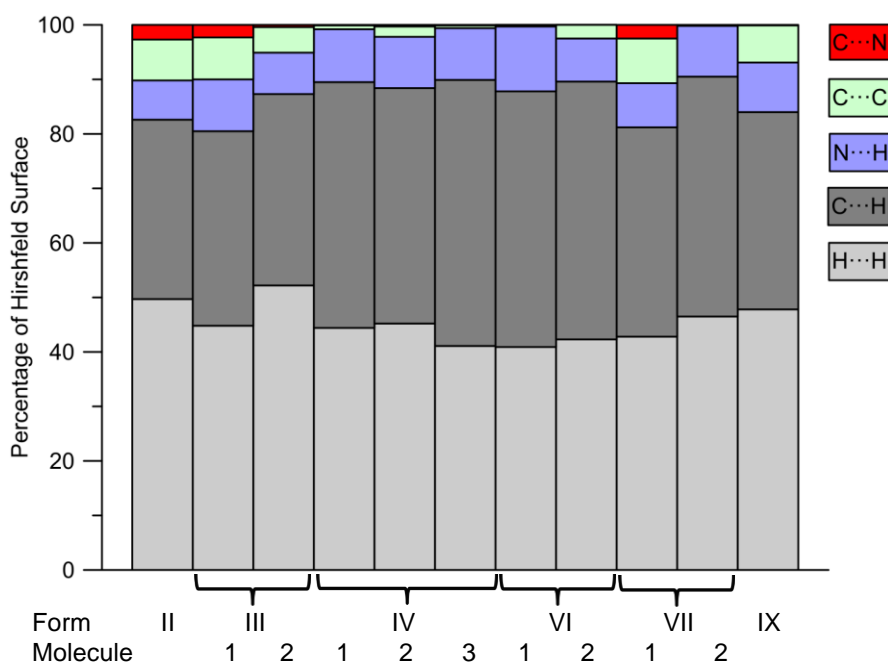

Figure 7. Fraction of the Hirshfeld surface of each acridine molecule in each polymorph associated with pairs of atoms. From the bottom: H···H (light grey), C···H (dark grey), N···H (lavender), C···C (green), C···N (red).

One might hope for general principles that would govern the packing of organic molecules in crystals, in the spirit of Pauling's rules[29] for ionic crystals. Obviously the problem of organic solids is much more complicated, because of the shapes of the constituent units, but it seems plausible to expect a similar concept of parsimony, that the immediate environment of a given molecule would be similar in different polymorphs, and similar for crystallographically inequivalent molecules in a $Z' > 1$ structure. The myriad set of environments and connections among acridine molecules in the six forms described above seems to present a strong counterexample to such speculation.

III. Thermal properties.

Studies of the thermal properties and crystal chemistry of acridine polymorphs are complicated by the fact that they have similar habits and occurrence domains, and close melting points. Furthermore, the polymorphs tend to crystallize concomitantly, so that several different forms may appear in one crystallization experiment. Kofler[3] published melting points of five modifications of acridine; four of them are in the range 109-110°C. The melting point of the fifth is reported as 106°C. This confluence of melting points complicates the elucidation of the thermal events visually in the hot stage microscope. Unfortunately, the crystallographic identity of those forms is not known. Our own measurements of melting points and heat of fusion, as well as measurements in the literature that can be correlated to specific forms, are summarized in Table 2.

Table 2: Melting point, density and heat of fusion of acridine polymorphs. Except as noted, all data are from this work, as detailed in Ref. 17 with sample results in SI Figures S3-S5.

Crystal Form	Hot Stage Microscope (°C) [a]	DSC peak(°C)	DSC onset (°C)	ΔH_{fus} (kJ mol^{-1})	Density (298K)
II	102-104.5	110.6	109.8	18.6	1.296 [ref 5]
III	110-110.5	109.8(0.6)[b]	106.8(0.50)[b]	20.33(1.50)[b]	1.285 [ref 10], 1.283 [6 and c]
IV	108.5-109.5		89±1 [ref 10]	16.2 [ref 10]	1.254[ref 10], 1.242[c]
VI			99 [ref 9]		1.254[c]
VII			101 [ref 9]		1.283[c]
VIII			109±1 [ref 10]		
IX	107.4-108.7	110.4	108.8	19.2	1.276 [ref 14]

[a] All crystals used were obtained by recrystallization from solution. Extreme values from all measurements.

[b] Averaged on a number of measurements; standard deviation of the average in brackets.

[c] Measured on a powder sample quenched from the melt; see SI.

There are several reports in the literature of transformations between solid forms. Lowde *et al.*[4] and Phillips[30] observed transformation from II to III at 45 °C or above, with increasing rapidity at higher temperature. In addition, Phillips[30] observed conversion from IV to III at about 70 °C. The only observed transformation between solid forms that did not end at III was by Braga *et al.*,[10] who observed transformation from form II to a previously undiscovered form VIII; like the elusive form V, this has not been reproduced by others. Nor has any solid-solid transformation been observed on cooling.

From the standpoint of thermodynamics, the most fundamental property of a polymorphic system is the relative stability (free energy) of the various forms, as a function of temperature and pressure. Consider first a system with two solid forms, A and B. If A has a lower free energy than B at all temperatures below their melting points, we say that the system is monotropic. In that case, one may obtain a sample of form B in a metastable state, and observe it to transform into form A, but a sample of form A will not spontaneously revert to form B at any temperature. The appearance of B when the melt is cooled does not necessarily mean it is more stable; it may be that B is kinetically preferred. On the other hand, if the free energies of the two forms cross as a function of temperature, the system is enantiotropic, and transformations from A to B and from B to A are allowed, depending on the temperature. That does not mean that such transformations will be observed; for example, the kinetics of transformation may be slow enough that the transformation is not observed. For example, while forms II and IV transform directly to III given sufficient time, they can be heated to their melting points which are significantly higher than the temperatures at which they transform to III.

To determine whether there is a thermodynamic transformation that is not observed because the kinetics are too slow, Burger and Ramberger[31] expressed a set of rules that are widely used in the analysis of polymorphic systems. One of these, the heat of fusion rule, states that a system is enantiotropic if the solid phase with the higher melting point has the lower heat of fusion. Inspection of Table 2 shows that this condition is satisfied both between II and III and between IX and III. Therefore, despite the fact that no transition from III to either of forms II or IX has been observed, we conclude that both are enantiotropically related to form III. However, we cannot conclude from experiment whether II or IX is the most stable low temperature form. Experimentally establishing the relative stabilities as a function of temperature within systems of

many (pairs of) polymorphs can be practically impossible, but the small energies involved make this a challenge to evolving computational methods.[16]

IV. Computational Survey

The ability to predict stable crystal structures based on molecular information alone is a long-sought goal, generally still elusive, although considerable progress has been made. A series of blind tests have been published, showing increasing success and ability to handle more complicated cases.[32] Successful methods depend on generating trial structures and ranking them according to their binding energy. The tradeoff between accuracy and computational efficiency and breadth of search in generating trial structures are two of the important heuristic principles in crystal structure prediction (CSP). As a rigid molecule known to have a large number of polymorphs, acridine is an interesting test case for CSP.

A decade ago, we used the program CrystalPredictor[33] to generate a crystal energy landscape, limited to one independent molecule in the asymmetric unit cell in the most common space groups. The molecular conformation was initially optimized using GAUSSIAN 03 at the MP2 level of theory with the 6-31G(d,p) basis set. This rigid conformation was used to generate the crystal structures, which were relaxed to a mechanically stable structure with DMACRYS.[34] The intermolecular forces were modelled using the FIT repulsion-dispersion potential[34] and a distributed multipole electrostatic model (GDMA2.2[35]) representing the MP2/6-31G(d,p) molecular charge density.

Fig. 8 shows the 61 CSP-generated $Z' = 1$ structures with lattice energy less than −93 kJ/mol, along with the lattice energies of the six experimental structures calculated by the same procedure. The method is notably successful in identifying the two known Z'=1 forms as two of

the lowest energy candidates, especially since IX was not known at the time of the CSP study. This gives confidence in the energy-ranking methodology, and raises the question: why have so *few* of the computer generated structures been observed? This is especially noteworthy since two thirds of the observed polymorphs of acridine have $Z' > 1$ and are therefore not found in the CSP study that produced Fig. 8. Possible answers include kinetic factors of crystallization and the influence of finite temperature on relative stability of different forms. The prediction of many more stable structures than are observed is a common feature of CSP, and there is considerable discussion as to whether these are possible undiscovered polymorphs or artefacts of the CSP method.[16]
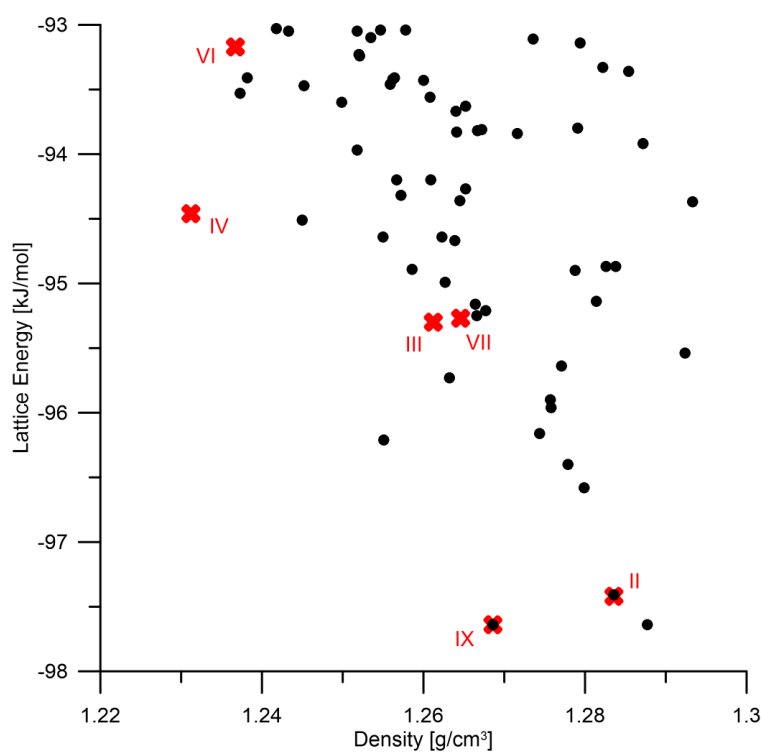

Figure 8. Summary of the crystal structure prediction study, showing the lattice energy and density of the low-energy computer generated $Z' = 1$ structures (black dots) and all observed forms (red crosses) of acridine. The lattice energies and densities correspond to the static ($T = 0$, $P = 0$) relaxed structures and so they can differ from the experimental values.

There is another predicted polymorph (CSP-A15), which tied with form IX for the minimum lattice energy, with a higher density, as shown in Fig. 8. Its predicted structure, HS, and HFP are presented in the supporting information, which shows that it has more C···C contacts and a different packing from any experimentally observed form.

It is important to determine how sensitive the CSP results are to the methodology used to compute lattice energies. Figure 9 shows that there is a significant re-ranking of the zero-temperature lattice energies when computed at the electronic level, using the dispersion-corrected density functional method PBE-TS, typically used for modelling organic polymorphs[36], as implemented in CASTEP[37]. Furthermore, using a recent improvement of the dispersion correction to include many-body terms[38] (PBE-MBD*) shuffles the relative stabilities by a comparable amount. It also makes A15 the least stable of the structures considered and reduces the spread of computed lattice energies of the known forms.
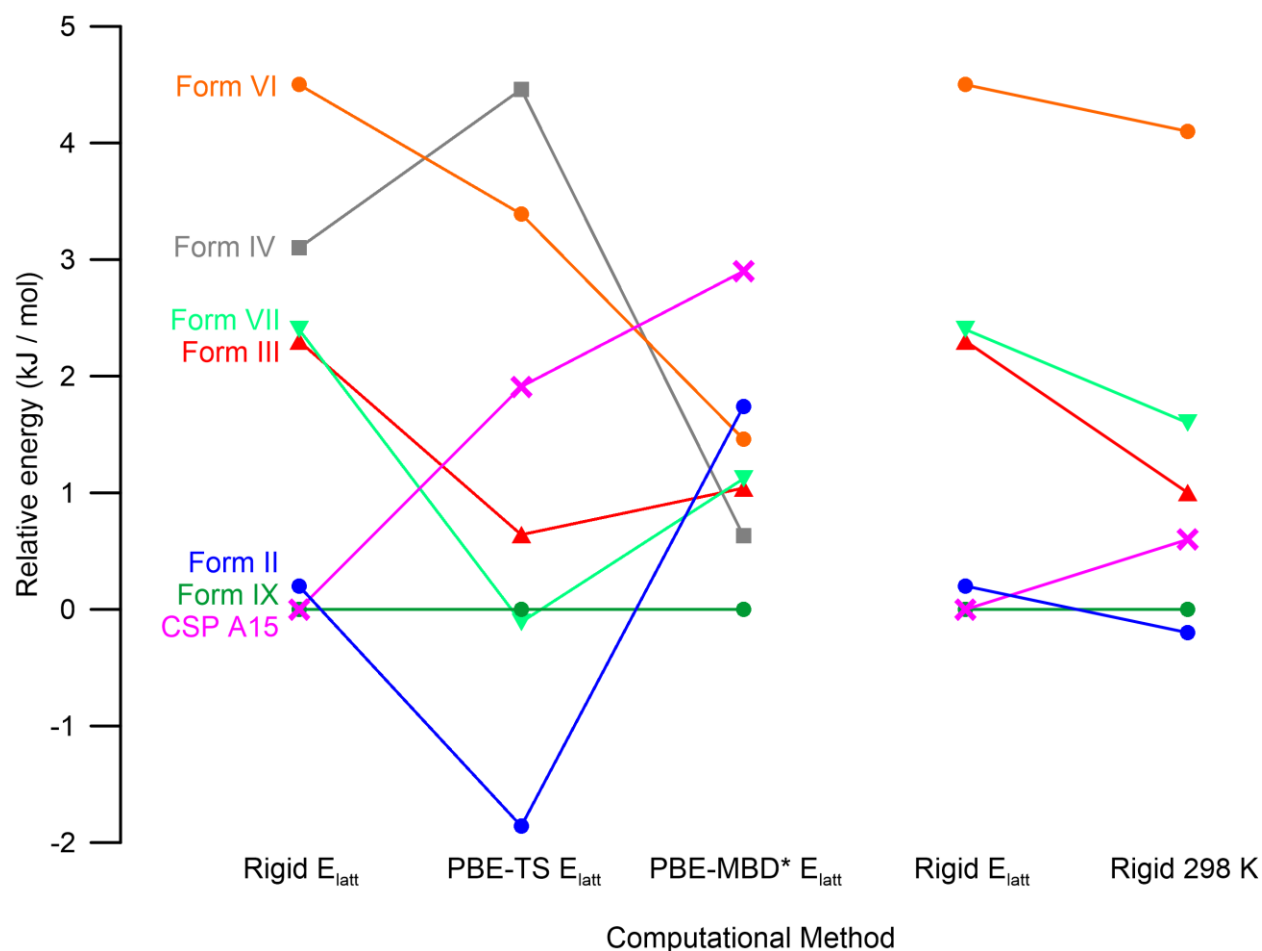
Figure 9: Crystal energies relative to form IX for the polymorphs and lowest energy unobserved CSP structure. On the left, E_{latt} are static (0 K) energies relative to infinite separation of the molecules, with "Rigid" denoting the intermolecular potential method used in the CSP (Fig. 8), "PBE-TS" denoting periodic electronic structure optimizations (SI), and "PBE-MBD*" the energy at that structure calculated with the MBD* dispersion correction. The right side compares the Helmholtz free energy estimated at 298 K within the rigid molecule harmonic approximation, based on the original intermolecular potential. (Form IV, with Z'=3, caused difficulties in evaluating all the low frequency modes; therefore results for this form are not available).

On the other hand, the experimental evidence is that form III is the most stable form, at least above 318 K. It is therefore worthwhile to extend estimates of the crystal energy to ambient temperature. This requires calculation of the vibrational contribution to the free energy, which can be estimated using an Einstein approximation of dispersionless optical lattice modes and a Debye approximation for the acoustic modes, calculated from the harmonic spring constants derived from the lattice energy model. The free energies evaluated using DMACRYS,[34] which holds the molecule rigid, are given in Fig. 9 (and Table S4). This shows that the entropic contribution brings the Helmholtz free energy of form III much closer to the two monomolecular forms that have the lowest computed lattice energy. Given the approximations in this model for the thermal motions of the molecules, it is entirely plausible that the free energy curves of IX and III, or II and III, cross below the melting point but above room temperature, strengthening the hypothesis derived from the thermal data, that the system is enantiotropic.

In any event, the sensitivity of the relative energies of the observed polymorphs to the representation of the molecular charge density, the dispersion model and any molecular flexibility, let alone the modeling of the effects of temperature, means that this polymorphic system is a challenge to computational methods. Whilst the most recent calculations suggest that A15 is no longer favored by thermodynamics, it is not so metastable that we can rule it out from being a plausible polymorph. The challenge is to devise an experiment to find it, such as a templating effect.[16]

V. Conclusion and Outlook.

In this review, we have summarized the current state of knowledge of the landscape of solid forms of acridine. An interesting aspect of this program was the discovery of a new form that

had been previously predicted in a computational search. We have seen that acridine has an unusually large number of polymorphs, and that their packing geometries significantly differ from one another. One of the pioneers of organic solid-state chemistry, A.I. Kitaigorodskii, described the situation as follows: "Acridine … has a 'hollow' in the middle, and is not, as a consequence, very convenient for packing…. That the shape of the molecule is inconvenient for packing seems to explain why the unit cells of other modifications contain more than one independent molecule in general positions. It is interesting to point out that all the polymorphic modifications have completely different structures."[39] Other apparently simple molecules with multiple polymorphs, such as benzidine and 1,8-dihydroxyanthraquinone could also be described as having a "hollow in the middle," and crystallize in a variety of space groups and a range of *Z'* values.[40] Indeed, since most molecules have a shape that is inconvenient for packing, they may well also be promiscuously polymorphic when subjected to a similar or greater screening effort. Thus the polymorphs of acridine provide a testbed for our ability to understand and predict polymorphism.

Supporting Information. A summary of crystal growth conditions, further comparison of crystal structures, IR and thermal characterization, simulated reference powder x-ray diffraction patterns, conversion of form II to III, and a mixture of forms III, IV, VI, and VII, the structure of the additionally predicted form of lowest energy, and details of the energy calculations.

Corresponding Author

*Email: pstephens@stonybrook.edu.

Present Addresses

† X-ray Science Division, Argonne National Laboratory, Lemont, IL 60439

§ Deceased.

Author Contributions

JB masterminded this project in his supervision of ES, his last graduate student, who performed the experimental work. SL and PWS determined the crystal structure of form IX. LSP performed the CSP and RG carried out the recent periodic electronic structure calculations. On JB's death, PWS and SLP completed the manuscript, preserving the tutorial style for which JB will be long remembered.

Abbreviations: CSD, Cambridge Crystal Structure Database; HS, Hirshfeld Surface; HFP, Hirshfeld Fingerprint, CSP, Crystal Structure Prediction calculations

References:

1.   Bernstein, J. *Polymorphism in Molecular Crystals;* Clarendon: Oxford, 2002.

2.   Schenk, H.; Peschar, R. Understanding the Structure of Chocolate. *Radiation Physics and Chemistry* **2004**, *71*, 829-835.

3.   Kofler, A. Zur Polymorphie organischer Stoffe: Acridin, Brenzcatechin, Diphenylamin und Korksäure. *Ber. Dtsch. Chem. Ges.* **1943**, *76*, 871-873.

4.   Lowde, R.D.; Phillips, D.C.; Wood, R.G. The Crystallography of Acridine. I. *Acta Cryst.* **1953**, *6*, 553-556.

5.   Phillips, D.C. The Crystallography of Acridine. Part II. The Structure of Acridine III. *Acta Cryst.* **1956**, *9*, 237-250.

6.   Phillips, D.C.; Ahmed, F.R.; Barnes, W.H. The Crystallography of Acridine. Part III. The Structure of Acridine II. *Acta Cryst* **1960**, *13*, 365-377.

7.   Herbstein, F.H.; Schmidt, G.M.J. The Crystal and Molecular Structures of Heterocyclic Compounds. I. The Analysis of the Crystal Structure of α-Phenazine. *Acta Cryst* **1955,** *8*, 399-405.

8.   Clarke, B.P.; Thomas, J.M.; Williams, J.O. The Relationship Between Crystallographic Structure and Luminescence in Single Crystals of Acridine. *Chem. Phys. Lett.* **1975**, *35*, 251-254.

9.   Mei, X.; Wolf, C. Formation of New Polymorphs of Acridine Using Dicarboxylic Acids as Crystallization Templates in Solution. *Cryst. Growth Des.* **2004**, *4*, 1099-1103.

10.   Braga, D.; Grepioni, F. Maini, L.; Mazzeo, P.P.; Rubini, K. Solvent-free preparation of co-crystals of phenazine and acridine with vanillin. *Thermochim. Acta* **2010**, *507-508*, 1-8.

11.   Kupka, A.; Vasylyeva, V.; Hofmann, D.W.M.; Yusenko, K.V.; Merz, K.   Solvent and Isotopic Effects on Acridine and Deuterated Acridine Polymorphism.   *Cryst. Growth Des.* **2012**, *12*, 5966-5971.

12.   Lusi, M.; Vitorica-Yrezabal, I.J.; Zaworotko, M.J.   Expanding the Scope of Molecular Mixed Crystals Enabled by Three Component Solid Solutions.   *Cryst. Growth Des.* **2015**, *15*, 4098-4103.

13.   Schur, E.; Bernstein, J.; Lemmerer, A.; Vainer, R.   Acridine 0.75-hydrate.   *Acta Cryst* **2011**, E*67*, o2761.

14.   Stephens, P.W.; Schur, E.; Lapidus, S.H.; Bernstein, J.   Acridine Form IX.   *Acta Cryst* **2019,** E75, 489-491.

15.   Groom, C.R.; Bruno, I.J.; Lightfoot, M.P.; Ward, S.C.   The Cambridge Structural Database.   *Acta Cryst* **2016**, B*72*, 171-179.

16.   Price, S.L.   Is zeroth order crystal structure prediction (CSP_0) coming to maturity? What should we aim for in an ideal crystal structure prediction code?   *Faraday Discuss.* **2018**, *211*, 9-30.

17.   Schur, E. The crystal chemistry of acridine.   Ph.D. Thesis, Ben-Gurion University of the Negev, 2013.

18.   Groth, P. *Chemische Krystallographie*; Verlag von Wilhelm Engelmann: Leipzig, 1919; pp 815-817.

19.   Musumeci, D.; Hunter, C.A.; McCabe, J.F.   Solvent Effects on Acridine Polymorphism. *Cryst. Growth Des.* **2010**, *10*, 1661-1664.

20.   Spackman, M.A.; Byrom, P.G.   A novel definition of a molecule in a crystal.   *Chem. Phys. Lett.* **1997**, *267*, 215-220.

21.   McKinnon, J.J.; Mitchell, A.S.; Spackman , M.A.   Hirshfeld Surfaces: A New Tool for Visualising and Exploring Molecular Crystals.   *Chem. Eur. J.* **1998**, *4*, 2136-2141.

22.   McKinnon, J.J.; Jayatilaka, D.; Spackman, M.A.   Towards quantitative analysis of intermolecular interactions with Hirshfeld surfaces.   *Chem Commun.* **2007**, 3814-3816.

23.   Spackman, M.A.; McKinnon, J.J.   Fingerprinting intermolecular interactions in molecular crystals.   *CrystEngComm* **2002**, *4*, 378-392.

24.   CrystalMaker® Software Ltd, Oxford UK.   http://www.crystalmaker.com (accessed March 20, 2019).

25.   Turner, M.J.; McKinnon, J.J.; Wolff, S.K.; Grimwood, D.J.; Spackman, P.R.; Jayatilaka, D.; Spackman, M.A.   CrystalExplorer17, **2017**. University of Western Australia. http://hirshfeldsurface.net (accessed March 20, 2019).

26.   Il'in, S.G.; Chetkina, L.A.; Golder, G.A.   Crystal and molecular structure of 2,3-dichloranthraquinone.   *Kristallografiya* **1975**, *20*, 1051-1053.

27.   Kay, M.I.; Okaya, Y.; Cox, D.E. A refinement of the Structure of the Room Temperature Phase of Phenanthrene, $C_{14}H_{10}$, from X-ray and Neutron Diffraction Data. *Acta Cryst.* **1971**, B*27*, 26-33.

28.   Geiger, D.K.; DeStefano, M.R.   Conformational differences and intermolecular C−H•••N interactions in three polymorphs of a bis(pyridinyl)-substituted benzimidazole. *Acta Cryst.* **2016**, C*72*, 867-874.

29. Pauling, L. The Principles Determining the Structure of Complex Ionic Crystals, *J. Amer. Chem. Soc.* **1929**, *51*, 1010-1026.

30. Phillips, D.C. The polymorphism of acridine. (conference abstract) *Acta Cryst,* **1954**, *7*, 649.

31. Burger, A.; Ramberger, R. On the Polymorphism of Pharmaceuticals and Other Molecular Crystals. I. *Mikrochimica Acta* **1979**, *72*, 259-271.

32. Reilly, A.M.; Cooper, R.I.; Adjiman, C.S.; Bahattacharya, S; Boese, A.D.; Brandenburg, J.G.; Bygrave, P.J.; Bylsma, R.; Campbell, J.E.; Car, R.; *et al.* Report on the sixth blind test of organic crystal structure prediction methods. *Acta Cryst.* **2016**, B*72*, 439-459.

33. Karamertzanis, P.G.; Pantilides, C.C. *Ab Initio* Crystal Structure Prediction – I. Rigid Molecules. *J. Comput. Chem.* **2005**, *26*, 304-324.

34. Price, S.L.; Leslie, M.; Welch, G.W.A.; Habgood, M.; Price, L.S.; Karamertzanis, P.G.; Day, G.M. Modelling organic crystal structures using distributed multipole and polarizability-based model intermolecular potentials. *Phys. Chem. Chem. Phys.* **2010,** *12*, 8478-8490.

35. Stone, A.J. Distributed Multipole Analysis: Stability for Large Basis Sets. *J. Chem. Theory Comput.* **2005,** *1*, 1128-1132.

36. Beran, G.J.O. Modeling Polymorphic Molecular Crystals with Electronic Structure Theory. *Chem. Rev.* **2016**, *116*, 5567-5613.

37. Clark, S.J.; Segall, M.D.; Pickard, C.J.; Hasnip, P.J.; Probert, M.I.J.; Refson, K.; Payne, M.C. First principles methods using CASTEP. *Z. Kristallogr.,* **2005**. *220* 567-570.

38.   Tkatchenko, A.; DiStasio, R.A.; Car, R.; Scheffler, M. Accurate and efficient method for many-body van der Waals interactions. *Phys. Rev. Lett.* **2012,** *108*, 236402.

39.   Kitaigorodskii, A.I. *Molecular Crystals and Molecules*; Academic Press: New York, 1973; pp. 72-73.

40.   Cruz-Cabeza, A.J.; Bernstein, J. Conformational Polymorphism. *Chem. Rev.* **2014**, *114*, 2170-2191.

For Table of Contents use: